International Journal of Applied Engineering Research
ISSN 0973-4562 Volume 10, Number 7 (2015) pp. 17137-17148

http://www.ripublication.com

Extended Kalman Filter Based Localization With Sonar Features Extracted By Grid Association For Mobile Robots

Se-Jin Lee, Nam-Hun Kim
Division of Mechanical and Automotive Engineering, Kongju National University, 1223-24 cheonan-daero, Seobuk-gu, cheon an-si, chungcheongnam-do, 330-710, South Korea
sejiny3@kongju.ac.kr, nhkim@kongju.ac.kr

Abstract

The SLAM or localization needs successful data association of the detected feature with landmarks. Well described features of the environment are essential for good data association. In this paper, the localization of the robot is executed by the extended Kalman filter (EKF) with given minimum landmarks of the environment. Consistent features for localization are extracted by using only sparse sonar data. Features are extracted by using a sonar data clustering from a footprint-association (FPA) method and a feature fitting from a least squares (LS) method to overcome challenges associated with sonar sensors, such as a wide beam aperture and a specular reflection effect. The extracted features are, also, evaluated as a post-processing through the probabilistic association which associates the extracted feature with the weighted average probability of the grids that are located within the area of position uncertainty of the feature. The proposed methods have been tested in a real home environment with a mobile robot.

Key words: Extended Kalman Filter, Footprint Association (FPA), Feature-based Mapping, Probabilistic Association Model, Sparse Sonar Data

Introduction

Mobile robot navigation requires certain vital information, including a representation of the environment, localization, path planning, and obstacle avoidance. Especially building a map of an environment can be the basis for other functions such as SLAM (simultaneous localization and map building) or localization problem for autonomous navigation. The consistency of SLAM or localization is led by good describe of the environment [1]. However, the robotic mapping has many problems [2]. A key challenge arises from the nature of the measurement noise. The second complicating

aspect of the robot mapping problem arises from the high dimensionality of the entities that are being mapped. Third, environments change over time.

Typical sensors for building environmental maps include vision systems and laser, infrared, and ultrasonic rangefinders. Researchers have used ultrasonic sensors extensively not only because these sensors are inexpensive but also because they provide direct depth information about object locations. Moreover, these sensors have a relatively long detection range and are unaffected by changes in light intensity. However, a sonar beam's specular reflection effect results in the multipath phenomenon [3]. This phenomenon, together with a wide beam aperture, makes it difficult to gather object locations using only a single sonar measurement.

Researchers commonly use two different approaches to build sonar maps. The first approach is grid-based and divides the environment into several two-dimensional (2-D) or three-dimensional (3-D) cells. Each cell is represented by the probability of its being occupied by an object [4]. Two typical techniques for building grid maps are the Bayesian updating model [5] and the orientation updating model [6,7]. Use of a grid map is very efficient for representing object locations, regardless of object shapes, but building and maintaining a map of a large space requires considerable memory.

The other common approach is feature-based and represents the environment using three basic primitive geometries: a line, a point, or an arc. Crowley (1985) developed one of the earliest feature-based approaches by introducing the concept of the composite local model [8]. This model used extracted straight-line segments from sets of sonar data and provided localization by matching them to a global line segment map stored previously. Wijk and Christensen (2000) later developed triangulation-based fusion (TBF) of sonar data, which delivers stable natural point landmarks [9]. Nagatani et al. (1999) developed the arc transversal median (ATM) method and an arc carving algorithm [10]. ATM and arc carving fused multiple sonar readings to improve azimuth resolution.

Leonard and Durrant-Whyte used a rotating sonar scanner to obtain densely scanned sonar data (Leonard, 1992), developing a simple threshold technique to extract regions of constant depth (RCDs) that were used to extract features such as lines and points [11]. Kleeman (1999) designed a new sonar system based on a digital signal processor (DSP) [12]. This system was able to produce accurate measurements and on-the-fly single cycle classification of planes, corners, and edges.

In this paper, the localization of the robot is executed by the extended Kalman filter (EKF) with given minimum landmarks of the environment. Consistent features for localization are extracted by using only sparse sonar data. Features are extracted by using a sonar data clustering from a footprint-association (FPA)method and a feature fitting from a least squares (LS) method to overcome challenges associated with sonar sensors, such as a wide beam aperture and a specular reflection effect. The extracted features are, also, evaluated as a post-processing through the probabilistic association which associates the extracted feature with the weighted average probability of the grids that are located within the area of position uncertainty of the feature. The proposed methods have been tested in a real home environment with a mobile robot.

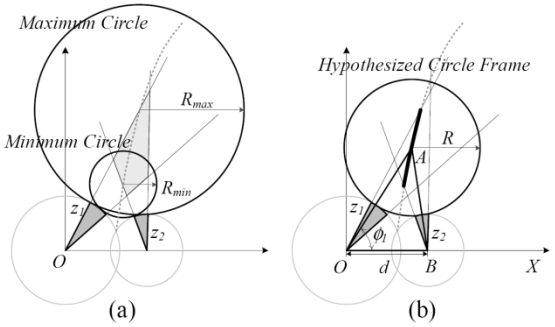

Figure 1: Hypothesized circles that are tangential to the two circles defined by the footprints: (a) possible radius range for the hypothesized circles without considering angle constraints, and (b) trace of virtual circles' centers that satisfy the angle constraints

The structure of this paper is as follows: Section 2 introduces the feature extraction method such as the FPA model and the LS fitting. Section 3 explores the EKF localization of robot pose. Section 4 presents the evaluation of the feature reliability through the probabilistic association. Section 5 illustrates the experimental setup and results. Finally, Section 6 draws conclusions and discusses future research topics.

Feature Extraction

Ultrasonic Sensor

Ultrasonic sensors can measure how far they are from the nearest object by using the elapsed time between a sonar beam's transmission and detection. However, they frequently fail to detect the nearest object. There are two possible explanations for this [3,7]. First, the object's surface may produce an echo amplitude that is too small to be detected by the receiver. Second, the echo pulse may be reflected from the receiver by a surface that is not perpendicular to the transducer axis. The latter, referred to as the specular reflection effect, happens more frequently. Since the surfaces of most real-world objects can be considered specular for ultrasonic sensors, this effect is almost always observed when the incidence angle is greater than half the beam's aperture [6].

The RCD method is one simple and powerful means of reducing both the specular reflection effect and angular uncertainty [11]. However, these methods cannot be used when data are sparsely scanned because neighboring sets of these data have few associations. Single rotating sonar is usually applied to gather densely scanned data, but single rotating sonar is not adequate for applications because it has a slow data acquisition speed. In addition, it requires a robot to stop when acquiring scanned data.

This study tested a sonar ring that gathered data quickly while a robot was in motion. In total, 8 sensors made by Murata were mounted on the sonar ring, one every 45º (the effective beam aperture). As mentioned above, sparsely scanned data do not allow rejection of incorrect data corrupted by the specular reflection effect, and cannot reduce the sonar beam's angular uncertainty. To compensate for these challenges, we

developed the data filter model by the sonar footprints acquired at different scanning steps and the probabilistic association model based on the occupancy probability grid map.

Footprint-Association Model

Sonar range readings generally contain considerable angular uncertainty because of their wide beam angle aperture. In addition, sonar sensors often produce false readings due to specular reflection of sound waves. Association of more than two sets of sonar data is therefore very important to prevent false readings and reduce angular uncertainties. We tested the FPA model as a data filter to overcome the problems of a wide beam aperture and a specular reflection effect. Application of the FPA model allows determination of whether two sonar footprints are associated with a line, a point, or an arc. Sonar footprints that correspond to a plane or a cylinder should all be tangential to that plane or cylinder, while sonar footprints that correspond to a corner or an edge should all intersect at a corner or edge point [11]. The FPA model basically estimates the possibility that two sets of sonar data originate from the same feature. For the example shown in Fig. 1, we can define two circles centered at sensor locations with radii equal to footprint range values, z_1 and z_2, and define the effective sonar beam aperture as each footprint's constraint angle, represented by the shaded fan shape. For more details on FPA model, please refer to our paper [13].

Least Squares Fitting

Given the large amount of spurious data coming from specular reflections and sonar artifacts, classical robust techniques such as RANSAC [14,15] or the Hough transform [16,17] seem very appropriate. However, because all sonar readings that correspond to the same feature are clustered together by using the FPA model in this paper, the information of features such as a line, a point, and an arc can be extracted from each cluster directly by using the LS fitting as Eq. (1).

$$M = (A^T A)^{-1} A^T b \tag{1}$$

In the line feature fitting, A matrix is $[x_i\ 1]$, b matrix is $[y_i]$, and M matrix is about the inclined angle and the intercept to y axis of fitted line. In the arc feature fitting, A matrix is $[x_i y_i]$, b matrix is $[-x_i^2\text{-}y_i^2]$, and M matrix is about the center and radius of the arc feature. For the point feature fitting, the point position is calculated from the numerical average of data. The parameters that characterize a line or point feature are the shortest distance and the visible direction with respect to the robot position; the parameters of anarc feature include the shortest distance and the visible direction from the robot position to the center of the arc, and the arc radius. The visible direction of a line feature, defined as normal direction of the line, represents which side of the line is visible.

Uncertainty Evaluation of a Feature

To evaluate the features through the probabilistic association, the position uncertainty of the features has to be estimated. The position uncertainty of a feature depends on both the measurement uncertainties of the sensor and robot's pose uncertainty. The

position of robot can be estimated as the robot motion model. Measurement uncertainties of the sonar sensing come from the range and angular error. We assume that the range and angular error of sensors are uncorrelated with each other, having zero mean Gaussian noise. We also assume the robot's pose uncertainty and the measurement uncertainties are uncorrelated with each other. For more details on the uncertainty estimation of the feature position, please refer to our paper [13].

Localization

Mobile robot localization is the problem of determining the pose of a robot relative to a given map of the environment. In this paper, the minimum crucial landmarks of the environment are given for the data association of the feature. The extended Kalman filter localization algorithm, EKF localization, is a special case of Markov localization. Kalman filters are Bayes filters that represent posteriors $p(\mu_t, \sum_t | z_t, u_t)$ with Gaussians. Gaussians are unimodal distributions that can be represented compactly by a small number of parameters. Its strength lies in its simplicity and in its computational efficiency [18]. Fig. 2 describes the extended Kalman filter algorithm.

In the Fig. 2, the function g in Line 2 is about robot motion model as Eq.(2).

$$g(u_t, \mu_{t-1}) = \mu_{t-1} + \begin{pmatrix} \frac{\Delta T}{2}\left(r_R\omega_{t,R} + r_L\omega_{t,L}\right)\cos\theta \\ \frac{\Delta T}{2}\left(r_R\omega_{t,R} + r_L\omega_{t,L}\right)\sin\theta \\ \frac{\Delta T}{2B}\left(r_R\omega_{t,R} - r_L\omega_{t,L}\right) \end{pmatrix} \tag{2}$$

G_t and V_t in Line 3 are computed as the Jacobians needed for the linearized motion model. M_t is determined as the motion noise covariance matrix from the control. Line 3, then, implement the motion update of the robot. The predicted pose after the motion is calculated as in Line 3 computes the corresponding uncertainty ellipse. The measurement update is realizedthrough Lines 4 to 17. It calculates a predicted measurement z^{*k}_t and the jacobianH^k_t of the measurement model. Using this Jacobian, the algorithm determinesS^k_t, the uncertainty corresponding to the predicted measurement z^{*k}_t. The correspondence variable *j(i)* is then chosen in line 10, by maximizing the likelihood of the measurement z^i_t given any possible landmark m_k in the map. The data association for line features is also enhanced by considering the direction of the line landmarks. The Kalman gain K^i_t is then calculated in Line 11. The estimate is updated in line 12 and 13, once for each feature. Finally, lines 15 and 16 set the new pose estimate.

1: Algorithm Extended Kalman Filter (μ_{t-1}, $\sum_{t-1}$, u_t, z_t, m):
2: $\mu_t^* = g(u_t,\mu_{t-1})$
3: $\sum_t^* = G_t\sum_{t-1}G_t^T + V_tM_tV_t^T$
4: for all observed features z_t^i do
5: for all landmarks k in the map m do
6: $z_t^{*k} = h(\mu_t^*)$
7: $H_t^k = \partial h(\mu_t^*)/\partial x$
8: $S_t^k = H_t^k\sum_t^* H_t^{kT} + Q_t$
9: endfor
10: $j(i) = argmax\ det(2\pi S_t^k)^{-0.5}$
$+ exp\{-0.5(z_t^i - z_t^{*k})[S_t^k]^{-1}(z_t^i - z_t^{*k})\}$
11: $K_t^i = \sum_t^* [H_t^{j(i)}]^T (S_t^{j(i)})^{-1}$
12: $\mu_t' = \mu_t^* + K_t^i(z_t^i - z_t^{*j(i)})$
13: $\sum_t' = (I - K_t^i H_t^{j(i)})\sum_t^*$
14: endfor
15: $\mu_t = \mu_t'$
16: $\sum_t = \sum_t'$
17: return $\mu_t, \sum_t$

Figure 2: The extended Kalman filter (EKF) localization algorithm with unknown correspondences.

Feature Evaluation Method

Almost all the line, point, and arc features can be generated at the position of real objects by using the FPA filtering and the LS fitting. However, there are unexpected features around a moving people or a complex environment due to wide beam width and specularity of sonar sensors. And the constructed features of the environment are hard to be flexible in changeable environment over time. In this paper, the feature evaluation method is developed by using the probabilistic association which uses the occupancy probabilities of grids in order to minimize phantom features and maintain dynamic features. For this association, the occupancy probability of grids is needed to associate the extracted feature with the weighted average probability of the grids that are located within the area of position uncertainty of the feature. The grid probability is calculated from the Bayesian updating model and the orientation probability model.

Grid Mapping

Bayesian probability map is composed of many grids that represent the robot's workspace, and each grid has an occupancy probability of an object. The grids within thesonar footprint, that are to be updated, are rearranged according to the distance from the transducer location. These grids are divided into two regions. The occupancy probability for the grid in the empty region should go down, while that in the occupied region should go up. An updating quantity of the occupancy probability is determined by using Bayes conditional probability theory according to the distance or angle of the grid from the sensor [19].

Bayesian model can supports a sound theoretical basis of a probability map. In the real application, however, it has a critical problem that seriously deteriorates the quality of the constructed map [7]. That is, the Bayesian model does not consider the specular reflection and the multi-path effects that frequently return incorrect range data.

To solve this problem, Lim and Cho developed a mapping model with ability to detect an occurrence of the specular reflection effect by evaluating the orientation probability in each grid [3,7]. In this model, the orientation probability is updated by using the specular reflection effect conversely. As the information is accumulated, the probability of the orientation corresponding to real object surface is continuously increased, while those of the rest orientations will be decreased. An occurring possibility of the specular reflection and the multi-path effects for each sonar range data can be probabilistically considered by using the orientation probabilities. It has been shown that the orientation model can construct a good quality map despite of the specular reflection effect [3,7].

Probabilistic Association for Feature Evaluation

The approach for the reliability evaluation of a feature is based on the occupancy probabilities of the grid map that is built using the hybrid map building model stated above. This approach can minimize the appearance of phantom features and maintain the dynamic features by using only sparse sonar data. Grid association is to associate the extracted feature with the weighted average probability of the grids that are located within the area of position uncertainty of the feature as shown in Fig. 3. The formula for the weighted average of the occupancy probability is written as:

$$a = \frac{\sum_{i=0}^{N} P_{Oi}(x,y) P_i(x,y)}{\sum_{i=0}^{N} P_i(x,y)} \tag{3}$$

Where a is the weighted average of the probabilities of grids in the area of feature position uncertainty, N is the number of grids in the ellipse of the position uncertainty. P_{Oi} is the occupancy probability of i_{th}grid,P_i is the probability of the Gaussian distribution of i_{th} grid. The formula of P_i at (x,y) is as follows:

$$P_i(x,y) = \frac{1}{2\pi\sqrt{\sigma_x^2\sigma_y^2(1-\rho^2)}} e^{-\frac{1}{2(1-\rho^2)}\left[\frac{x^2}{\sigma_x^2}+\frac{2\rho xy}{\sigma_x\sigma_y}+\frac{y^2}{\sigma_y^2}\right]} \tag{4}$$

whereσ_x and σ_y are the standard deviations of x and y respectively, ρ is the correlation coefficient for x and y. These variables can be obtained from the covariance matrix of the feature position uncertainty, and has of the form:

$$C = \begin{pmatrix} \sigma_x^2 & \rho\sigma_x\sigma_y \\ \rho\sigma_x\sigma_y & \sigma_y^2 \end{pmatrix} \tag{5}$$

For more details on the uncertainty estimation of the feature position, please refer to our paper [20].

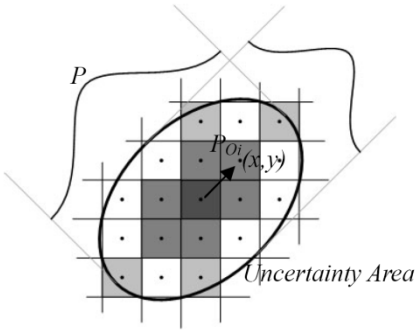

Figure 3: Ellipse of a point feature position uncertainty. The weighted average of the occupancy probability is found using grids in the area of feature position uncertainty.

Experimental Results

The methods as developed above have been implemented and tested in a real home environment with real robot. The robot is Pioneer 3-DX that has a ring of 8 Murata ultrasonic sensors with the height of 63cm. The transitional and rotation speeds of the robot are 0.2m/s and 15deg/s.

Fig. 4 shows a real home environment that is composed of fabric bed, table, clothes chest, bookshelf, and windows. The filtered sonar data around fabric bed is sparser than around other objects and the ultrasonic toward the bed can pass the bed because the height of the sensor is higher than it of the bed. The size of the room is 6.8m×5.9m space. Thin lines are the environment shape. Thick lines are the selected line landmarks among the environment. Gray short lines are the visible direction of the line landmarks. Thick small circles are the selected point landmarks. Thick arc is the selected arc landmark. The numbers of line and point landmarks are 11 and 3, respectively. Thin small circle is the start station of the robot. Dotted lines are the odometry path of the robot. Medium lines are the estimated path of the robot by the EKF filter. The robot was run following the thick lines in Fig. 4 using a remote controller with the EKF localization. The total trajectory of the robot was around 39.9m with 4031 steps, lasting around 6.7 minutes.

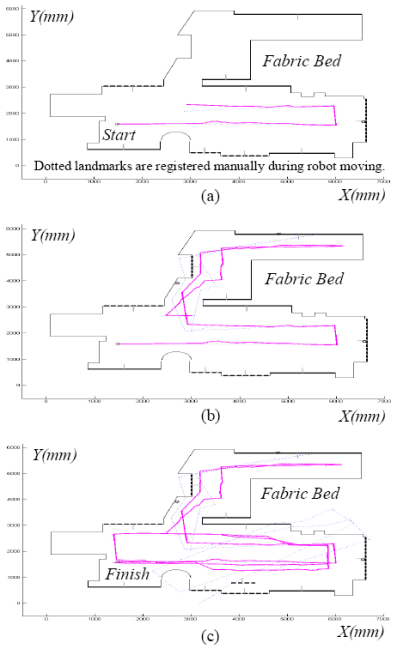

Figure 4: Real home environment and selected landmarks, odometry and estimated path of the robot during (a) 1.1, (b) 3.3, and (c) 6.7 minutes of the trajectory

During the robot motion, the sonar ring wasacquiring range scans at average frequency of 10 Hz. 3 line and 1 point landmarks are registered manually during 1.1 minutes in Fig. 4(a). And 1 line and 2 point landmarks are registered additionally during 3.3 minutes in Fig. 4(b). In Fig. 4(c), 1 line landmark is registered during 6.7 minutes, because the chair is located at the middle of low boundary. The number of data association times with 14 landmarks is 384. The pose error of x, y, and heading angle at final location are 8.8cm, 3.4cm, and 0.06rad, respectively.

Fig. 5 shows the extracted features and the grid map during the first 3.1 minutes of the trajectory. Gray grids are the occupancy probabilistic grid map by using the filtered sonar data and the size of cell is 15cm×15cm. Fig. 5(a) shows all extracted features by LS fitting before applying the probabilistic association and Fig. 5(b) shows the evaluated features by the probabilistic association with the grid map. Although the wrong features are generated at the free space due to moving people and sonar's wide beam width and specularity in Fig. 5(a), the reliable features through the probabilistic association are remained at the position of real objectsand the features in free space are removed clearly in Fig. 5(b).

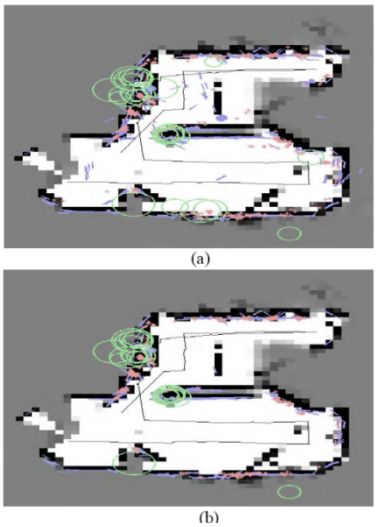

Figure 5: Occupancy grid map and features during the first 3.1 minutes of the trajectory (a) before applying the probabilistic association and (b) after applying the probabilistic association.

Fig. 6 shows the extracted features and the grid map during total minutes of the trajectory. Fig. 6(a) shows all extracted features by LS fitting and Fig. 6(b) shows the evaluated features by the probabilistic association with the grid map. In Fig. 6, the chair marked by dotted circle is located at the middle of low boundary after first 3.1 minutes of the trajectory. The new features on the chair are generated and evaluated, although that position was empty region at the last state of Fig. 6. Using the technique described in section 4.2, the sonar features on new dynamic object can be generated.

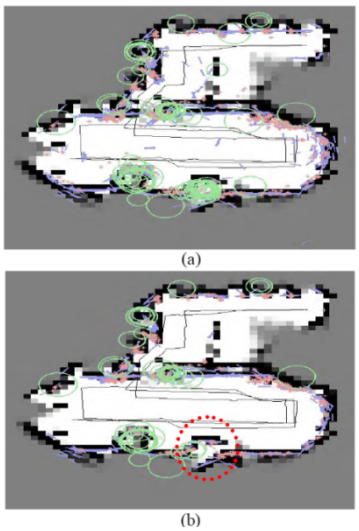

Figure 6: Occupancy grid map and features during the total minutes of the trajectory (a) before applying the probabilistic association and (b) after applying the probabilistic association

Conclusions

In this paper, measurement noises of the sonar such as wide beam width and specular reflection phenomenon are overcome through the FPA model. And the problems caused by sonar specularity, moving people, and dynamic object are solved through the probabilistic association model. By using these techniques, the map configuration of given environment can be kept consistently. By using sonar features, the localization of the robot is executed successfully by the extended Kalman filter (EKF) with given minimum landmarks of the environment. The features resulted by the FPA and probabilistic methods can be very useful for the SLAMproblem with only sonar sensors. In the future, the algorithm of autonomous feature joining and landmark registration will be developed.

References

[1] Lu, F. and Milios,E.,1997, "Globally Consistent Range Scan Alignment for Environment Mapping," *Autonomous Robots*, Vol. 4, pp. 333-349.

[2] Thrun, S., 2002, *Robotic Mapping: A Survey*, Morgan Kaufmann.

[3] Lim,J. H.and Cho,D.-W.,1994, "Specular reflection probability in the certainty grid representation," *Trans. of the ASME,*Vol. 116, pp. 512-520.

[4] Elfes, A. and Moravec, H. P.,1985,"High resolution maps from wide angle sonar," *IEEE Int. Conf. on Robotics and Automation*, pp. 116-121.

[5] Cho, D.-W.,1990, "Certainty grid representation for robot navigation by a Bayesian method," *ROBOTICA*Vol. 8, pp. 159-165.

[6] Lim, J. H.,1994, "Map construction, exploration, and position estimation for an autonomous mobile robot using sonar sensors," *PhD dissertation*, Pohang Institute of Science and Technology, Korea.

[7] Lim,J. H.and Cho,D.-W.,1996, "Multipath Bayesian map construction model from sonar data," *ROBOTICA*Vol. 14,pp. 527-540.

[8] Crowley,J. L., 1985, "Navigation for an intelligent mobile robot," *IEEE J. of Robotics and Automation*, RA-1(1), pp. 31-41.

[9] Wijk, O. and Christensen, H. I.,2000, "Triangulation-based fusion of sonar data with application in robot pose tracking," *IEEE Trans. on Robotics and Automation*, Vol. 16(6),pp. 740-752.

[10] Nagatani, K., Lazar,N. A., and Choset,H.,1999, "The arc-transversal median algorithm: An approach to increasing ultrasonic sensor accuracy," *IEEE Int. Conf. on Robotics and Automation*, pp. 644-651.

[11] Leonard,J. J.,1992,*Direct Sonar Sensing for Mobile Robot Navigation*, Dordrecht, The Netherlands: Kluwer Academic Publishers.

[12] Kleeman,L.,1999, "Fast and accurate sonar trackers using double pulse coding," *IEEE/RSJ International Conference on Intelligent Robots and Systems*, pp. 1185-1190.

[13] Lee,S.-J., Lim,J.-H., Cho,D.-W., Kang,C. U., and Chung,W. K.,2005, "Feature Based Map Building Using Sparse Sonar Data," *IEEE/RSJ Intl. Conf. on Intelligent Robots and Systems*, pp. 492-496.

[14] Fischler, M. A. and Bolles, R. C.,1981,"Random sample consensus: A paradigm for model fitting with applications to image analysis and automated cartography,"*Comm. Assoc. Comp. Mach.*, Vol 24(6), pp. 381-395.

[15] Hartley, R. and Zisserman,A.,2000,*Multiple View Geomety in Computer Vision*, Cambridge, UK: Cambridge University Press.

[16] Ballard,D. H. and Brown,C. M.,1982,*Computer Vision*, Englewood Cliffs, NJ: Prentice Hall.

[17] Tardos, J. D., Neira, J., Newman,P. M., and Leonard,J. J.,2002,"Robust Mapping and Localization in Indoor Environments Using Sonar Data,"*The Int. J. of Robotics Research*, Vol. 21(4), pp. 311-330.

[18] Thrun, S., Burgard, W., and Fox, D.,2005,*Probabilistic Robotics*, The MIT Press.

[19] Cho, D. -W. and Moravec, H. P.,1989, "A Bayesian Method for Certainty Grids,"*AAAI Spring Symposium on Robot Navigation*, Stanford, CA, pp. 57-60.

[20] Lee, S.-J., Lee,Y., Lim,J.-H., Kang,C.-U., Cho,D.-W., Chung,W.-K. and Yun,W.-S., 2006,"Evaluation of Features through Grid Association for Building a Sonar Map," *The 2006 IEEE ICRA*, pp. 2615-2620.